

Exploration of a modified density dependence in the Skyrme functional

J. Erler¹, P. Klüpfel², P.-G. Reinhard¹

1) *Institut für Theoretische Physik II, Universität Erlangen-Nürnberg, Staudtstrasse 7, D-91058 Erlangen, Germany*

2) *Science Institute, University of Iceland, Dunhaga 3, IS-107 Reykjavik, Iceland*

(Dated: Received: date / Revised version: date)

A variant of the basic Skyrme-Hartree-Fock (SHF) functional is considered dealing with a new form of density dependence. It employs only integer powers and thus will allow a more sound basis for projection schemes (particle number, angular momentum). We optimize the new functional with exactly the same adjustment strategy as used in an earlier study with a standard Skyrme functional. This allows direct comparisons of the performance of the new functional relative to the standard one. We discuss various observables: bulk properties of finite nuclei, nuclear matter, giant resonances, super-heavy elements, and energy systematics. The new functional performs at least as well as the standard one, but offers a wider range of applicability (e.g. for projection) and more flexibility in the regime of high densities.

PACS numbers: 21.10.Dr, 21.10.Ft, 21.60.-n, 21.60.Jz

I. INTRODUCTION

Self-consistent mean-field models have grown to be a major tool in the theoretical description of nuclei and nuclear dynamics. There are several approaches to nuclear SCMF from which the most widely used are the Skyrme-Hartree-Fock (SHF) model [1], the Gogny force [2], and the relativistic mean-field model (RMF) [3, 4]. All these models employ effective interactions which provide reliable nuclear structure properties and low-energy excitations at the level of a mean-field description. The general strategy for constructing nuclear energy functionals for high-quality calculations is to deduce the formal structure from principle considerations [5] and to rely on a phenomenological adjustment of the model parameters. There is a long history of SHF development and optimization (for recent reviews see [1, 6]) and yet, there is still demand for improvement as can be seen from the many recent updates of the parameterizations, for recent examples from SHF see e.g. [7–11]. In spite of all these activities, there remain several open problems which touch the structure of present days SHF functionals [12]. One such point is the way in which the density dependence is modeled. It used to start from adding to the zero-range two-body term a “three-body term” associated with a density dependence $\propto \rho^3$ where ρ is the local nucleon density [13]. This was found to be too restrictive and has been generalized to a profile $\propto \rho^{2+\alpha}$ with $\alpha \sim 0.16-0.3$ in order to allow a better description of fission barriers and monopole oscillations [14]. Since then, this form for the one density dependent term was carried forth unchanged. The reason is that most empirical information on nuclear structure is associated with densities near bulk equilibrium density $\rho_0 \approx 0.16 \text{ fm}^{-3}$.

Systematic information in a wide range of densities has not yet been acquired contrary, e.g., to the case of modeling liquid ^3He [15, 16]. Nonetheless, the traditional form $\propto \rho^{2+\alpha}$ is an arbitrary guess, it is rather rigid what extrapolation to the low density region (=weak binding) is concerned, and in particular, the non-analytical behavior for non-integer α turns out to be a great hindrance for particle-number projection [12, 17]. It is the aim of this paper to present and discuss an alternative form of the density dependence for the SHF functional which is built in the form of rational approximants using only integer powers of ρ . This will then provide a SHF functional which can safely be used in projection schemes, particularly for particle-number projection [18]. Moreover, we will exploit the generalized form to explore the effect of varied density dependence on bulk properties of finite nuclei. The new SHF functional is calibrated and investigated with the techniques of least-squares fitting and the basic data set as developed in a previous large scale study [10]. This allows a direct comparison with the former results using the traditional density dependence and it provides the same systematics of variations.

II. THE ENERGY FUNCTIONAL

The SHF functional is formulated in terms of the following local densities and currents (for details see [1, 10] and appendix A): density ρ_q , kinetic-energy density τ_q , spin-orbit density \mathbf{J}_q , current \mathbf{j}_q , spin density σ_q , and pair density ξ_q , where the index $q \in \{p, n\}$ labels protons and neutrons; total densities are denoted as $\rho = \rho_p + \rho_n$ and similarly for the other densities. Starting point is an expression of the total energy

$$E = E_{\text{kin}} + \int d^3r \mathcal{E}_{\text{Sk}}(\rho, \tau, \vec{j}, \vec{J}) + E_C(\rho_p) + E_{\text{pair}} - E_{\text{cm}} \quad (1a)$$

$$E_{\text{kin}} = \int d^3r \left(\frac{\hbar^2}{2m_p} \tau_p + \frac{\hbar^2}{2m_n} \tau_n \right) \quad (1b)$$

$$\mathcal{E}_{\text{Sk}} = \mathcal{E}_{\text{Sk,tb}}(\rho, \tau, \vec{j}) + \mathcal{E}_{\text{Sk,ls}}(\rho, \vec{J}) + \mathcal{E}_{\text{Sk,dens}}(\rho) \quad (1c)$$

$$\mathcal{E}_{\text{Sk,tb}} = \frac{b_0}{2} \rho^2 - \frac{b'_0}{2} \sum_q \rho_q^2 + b_1(\rho\tau - \vec{j}^2) - b'_1 \sum_q (\rho_q \tau_q - \vec{j}_q^2) - \frac{b_2}{2} \rho \Delta \rho + \frac{b'_2}{2} \sum_q \rho_q \Delta \rho_q \quad (1d)$$

$$\mathcal{E}_{\text{Sk,dens}} = \left[\frac{b_3}{2} \rho^2 - \frac{b'_3}{2} \sum_q \rho_q^2 \right] \rho^\alpha + \left[\frac{\tilde{b}_3}{2} \rho^2 - \frac{\tilde{b}'_3}{2} \sum_q \rho_q^2 \right] \frac{\alpha_{\text{inv}} \rho + \beta_{\text{inv}} \rho^2}{1 + \alpha_{\text{inv}} \rho} \quad (1e)$$

$$\begin{aligned} \mathcal{E}_{\text{Sk,ls}} = & -b_4(\rho \nabla \cdot \vec{J} + (\nabla \times \vec{\sigma}) \cdot \vec{j}) - b'_4 \sum_q (\rho_q (\nabla \cdot \vec{J}_q) + (\nabla \times \vec{\sigma}_q) \cdot \vec{j}_q) \\ & - \eta_{\text{tIs}} \left(\frac{1}{16} (t_1 x_1 + t_2 x_2) \vec{J}^2 - \frac{1}{16} (t_1 - t_2) \sum_q \vec{J}_q^2 \right) \end{aligned} \quad (1f)$$

$$E_C = \frac{1}{2} e^2 \int d^3r d^3r' \rho_p(\vec{r}) \frac{1}{|\vec{r} - \vec{r}'|} \rho_p(\vec{r}') - \eta_{\text{Cex}} \frac{3}{4} e^2 \left(\frac{3}{\pi} \right)^{\frac{1}{3}} \int d^3r [\rho_p(\vec{r})]^{\frac{4}{3}} \quad , \quad (1g)$$

$$E_{\text{pair}} = \frac{1}{4} \sum_{q \in \{p, n\}} V_{\text{pair}, q} \int d^3r \xi_q^2 \left[1 - \frac{\rho}{\rho_{0, \text{pair}}} \right] \quad , \quad (1h)$$

$$E_{\text{cm}} = \frac{1}{2mA} \langle \hat{P}_{\text{cm}}^2 \rangle \quad , \quad \text{after variation.} \quad (1i)$$

From this total energy it is straight forward to derive the corresponding mean field equations by variation with respect to the single-nucleon wavefunctions and the pairing amplitudes.

A. The Skyrme energy functional

The Skyrme functional in the narrower sense is given by the Skyrme energy density \mathcal{E}_{Sk} comprised in the terms (1d–1f). The parts (1d) and (1f) carry the zero-range two-body terms including effective mass and spin-orbit couplings. All density dependence is collected in the term (1e). Its first contribution $\propto b_3, b'_3$ represents the traditional density dependence. The second contribution adds the essential new piece where the density dependence is modeled as a rational approximant. Note that this term employs only integer powers of ρ . This new form has thus the great advantage that it complies with particle-number projection. The idea is that this rational density dependence replaces the traditional dependence ρ^α . Thus we can switch the models by the coefficients. The traditional model is recovered by setting $\tilde{b}_3, \tilde{b}'_3 = 0$. The new model with rational density dependence uses non-zero $\tilde{b}_3, \tilde{b}'_3$ and switches off the traditional form with $b_3, b'_3 = 0$. Both forms associate the same density dependence to isoscalar and isovector terms. One may introduce more isovector freedom in the density dependent terms by using all terms, i.e., $\tilde{b}_3, \tilde{b}'_3 \neq 0$ together with

$b_3, b'_3 \neq 0$, but fixing $\alpha = 1$ to maintain the crucial feature that only integer powers of ρ are used. We will consider this extended option to explore the impact of (isovector) density dependence.

One may wonder why one needs such an involved rational form. A straight-forward approach would start with a mere Taylor expansion for the density dependence, e.g. $\propto \rho^2 [c_1 \rho^1 + c_2 \rho^2 + c_3 \rho^3 \dots]$. It turns out that this simple form is not able to reproduce the appropriate density dependence at low densities. The form ρ^α with small α performs, in fact, very well in this regime which explains its great success in the development of the SHF functionals. It is clear that the non-analytical ρ^α resists a straightforward Taylor expansion. The rational approximant is much more flexible and allows a good fine tuning also in the low-density regime.

The spin-orbit part of the SHF functional (1f) contains the tensor term with a switch factor η_{tIs} . The importance of and the need for this term is still a matter of debate [9, 10, 19]. The new parameterization developed here will employ the tensor terms, i.e. we deal with $\eta_{\text{tIs}} = 1$.

The Skyrme energy as given above contains the minimum number of time-odd terms which are needed to make the functional Galilean invariant [20]. There are many more time odd terms conceivable at the level of given functionals [1, 21, 22]. They are unimportant for even-even nuclei and will be ignored here.

The parameters b_i, b'_i used in the above definition of the Skyrme functional are chosen to give a most convenient

formulation of the energy functional, the corresponding mean-field Hamiltonian and residual interaction. Traditional expressions for the Skyrme functional use a different labeling. The relation to the standard Skyrme parameters t_i , x_i [1, 6, 20, 23] is given in appendix B.

B. Additional terms

The direct Coulomb term employs the mere proton density ρ_p and not the charge density which would be obtained from folding with the nucleonic charge distributions [24]. The difference is, in principle, sizeable for heavy nuclei, but easily compensated for by the other terms in the functional. We keep the above form for reasons of simplicity.

The Coulomb-exchange functional, the second term in (1g), has been made switchable by the parameter η_{Cex} . Unfortunately, the LDA for Coulomb exchange invokes a non-integer power of density which, again, inhibits particle-number projection. Thus we will omit this contribution by using $\eta_{\text{Cex}} = 0$ in the new parameterizations. Coulomb exchange is a small contribution and the missing term will easily be taken up by the other terms in the functional.

For the center-of-mass correction E_{cm} , we use the standard recipe as given in eq. (1i). Note the comment “after variation” therein. The E_{cm} is, in fact, the expectation value of a two-body operator which makes the mean-field equations in fully variational treatment rather cumbersome. As E_{cm} is a small correction, we evaluate it (non-variational) at the end of the mean-field calculation for then given single-particle wavefunctions.

The pairing functional (1h) contains a continuous switch, the parameter $\rho_{0,\text{pair}}$ where volume pairing is recovered for $\rho_{0,\text{pair}} \rightarrow \infty$ and surface pairing for $\rho_{0,\text{pair}} = 0.16 \text{ fm}^{-3}$. We will use $\rho_{0,\text{pair}}$ as a free parameter and usually obtain a form of the pairing functional which stays in between the extremes of volume and surface pairing [10].

C. Adjustment strategy and the variants in this survey

The parameters of the new SHF functional are determined by phenomenological adjustment as it is done for most SHF functionals. We employ exactly the same fit strategy and data as used in a recent large scale survey [10]. The data set has been selected to cover spherical nuclei with negligible correlation effects [25] which amounts to isotopic and isotonic chains of semi-magic nuclei (leaving out the mid-shell regions). As leading observables we consider binding energy and key pattern of the nuclear charge distribution: r.m.s. radius, diffraction radius and surface thickness [26]. For pairing properties we include the three-point gaps as deduced from the odd-even staggering of binding energies and for determining

name	model	fit data
SV-bas	$b_3, b'_3 \neq 0; \tilde{b}_3, \tilde{b}'_3 = 0$	std, $a_{\text{sym}}, \kappa, m^*/m$
RD-bas	$b_3, b'_3 = 0; \tilde{b}_3, \tilde{b}'_3 \neq 0$	std, $a_{\text{sym}}, \kappa, m^*/m$
RM-bas	$b_3, b'_3 \neq 0, \alpha = 1; \tilde{b}_3, \tilde{b}'_3 \neq 0$	std, $a_{\text{sym}}, \kappa, m^*/m$
SV-min	$b_3, b'_3 \neq 0; \tilde{b}_3, \tilde{b}'_3 = 0$	std
RD-min	$b_3, b'_3 = 0; \tilde{b}_3, \tilde{b}'_3 \neq 0$	std
RM-min	$b_3, b'_3 \neq 0, \alpha = 1; \tilde{b}_3, \tilde{b}'_3 \neq 0$	std

TABLE I: Definition of the parameterizations. The acronym RD stands for “Rational Density dependence” and RM for “Rational and More density dependence”. The entry “std” in the rightmost column indicates that the standard pool of fit data from finite nuclei is used [10]. Further entries, if present, indicate the nuclear matter properties which had been added to the standard set: a_{sym} = symmetry energy at bulk equilibrium (fixed at 30 MeV), κ = isovector sum-rule enhancement factor (fixed at 0.4), m^*/m = effective nucleon mass (fixed at 0.9).

the spin-orbit parameters we take into account selected spin-orbit splittings in doubly-magic nuclei. The actual adjustment is performed with straightforward least-squares techniques. These allow not only to determine the optimal parameters but also provide a measure for the uncertainty on the parameters and deduced observables [10, 27].

Table I shows the variants of the model studied in the following. The parameterizations SV-bas and SV-min rely on the standard SHF functional (note the $\tilde{b}_3, \tilde{b}'_3 = 0$) and were presented in great detail in [10]. SV-min results from a straightforward fit to the data from finite nuclei. The “min” stands for minimization of the quality measure χ^2 . This straightforward fit turns out to leave large uncertainties on some nuclear matter properties, and with it on nuclear giant resonance excitations. Therefore a restricted fit was performed where some bulk properties (see last column of table I) were fixed to commonly accepted values [1] which turn out to yield a very good description of giant resonances in ^{208}Pb . (The actual values which were kept fixed can be read off from figure 2.) This led to SV-bas where “bas” stands for base point because it was used in [10] as the origin for a systematic variation of bulk properties.

The new parameterizations take over the twofold strategy, free fit “min” and bulk restricted fit “bas”. We consider first the new density dependent term alone leading to the parameterizations RD-min and RD-bas. A more flexible density dependence is explored by allowing also the traditional density dependent term with fixed $\alpha = 1$. These are the parameterizations RM-min and RM-bas. Comparing the RD forces with the RM forces allows to learn more about the impact of isovector freedom in the density dependence.

We also compare with results from established SHF parameterizations: SkM* as a widely used old standard [14] which for the first time managed to deliver accept-

able surface energy and fission barriers; SLy6 which had been developed with a bias to neutron rich nuclei and neutron matter aiming at astrophysical applications [28]; SkI3 adding the freedom of an isovector spin-orbit force to obtain an improved description of isotopic shifts of r.m.s. radii in neutron rich Pb isotopes [29]; BSk4 from [30] as representative of the series of fits to all available nuclei [7] having an effective mass of $m^*/m = 0.92$ which is best comparable to the new forces here. Each one of these parameterizations uses different sets of fit data, bias and constraints. Nonetheless, they yield very similar results for nuclear bulk properties, but differ in extrapolations and more detailed observables [1]. Note that these traditional parameterizations are taken as given. It is not possible to determine their extrapolations errors in the results discussed later on.

The detailed parameters for the four new parameterizations are given in table II in appendix B. The extended version RM-min and RM-bas have a negligible isoscalar parameter b_3 . A value of zero could be enforced without any significant change in quality and other properties. However, the isovector parameter b'_3 is large, accompanied by a similarly large change in the complementing \tilde{b}'_3 . The extended functional thus exploits its freedom, as expected, to tune isovector properties. The parameters α_{inv} and β_{inv} are very similar for all four forces. The typical value of $\alpha_{\text{inv}} \approx 15 \text{ fm}^3$ means that the functional has a simple pole at $\rho = -1/15 \text{ fm}^{-3} \approx -0.067 \text{ fm}^{-3}$. This means that the functional is not strictly analytical. But this pole is safely outside the range of possible single particle transition densities (whose absolute value is $\rho(\vec{r})$ but which can take any complex phase [17, 18]) and thus the integrations in the projection schemes stay fully in the analytical regime.

III. RESULTS AND DISCUSSION

A. Quality with respect to bulk observables

Figure 1 shows the average errors for the four basic nuclear bulk properties. It is to be noted that the older parameterizations (SkM*, SLy6, SkI3, and BSk4) were tuned with different data and strategies than used here. This explains, e.g., the larger energy error for SkI3 which was fitted to relative energy deviation and so has more bias to light nuclei, or the larger error on the diffraction radius R for BSk4 which was not included in its fitting set. Nonetheless, comparing with the traditional parameterizations, the progress in accuracy over the years becomes obvious. The parameterizations RD-bas and RD-min using the new density dependence provide a description which is very much comparable to the SV-bas and SV-min which were fitted to the same pool, of data but using the traditional density dependence of the Skyrme functional. The step to RM-min and RM-bas adds more flexibility and necessarily should deliver an improved description. A reduction of errors is indeed seen, but the

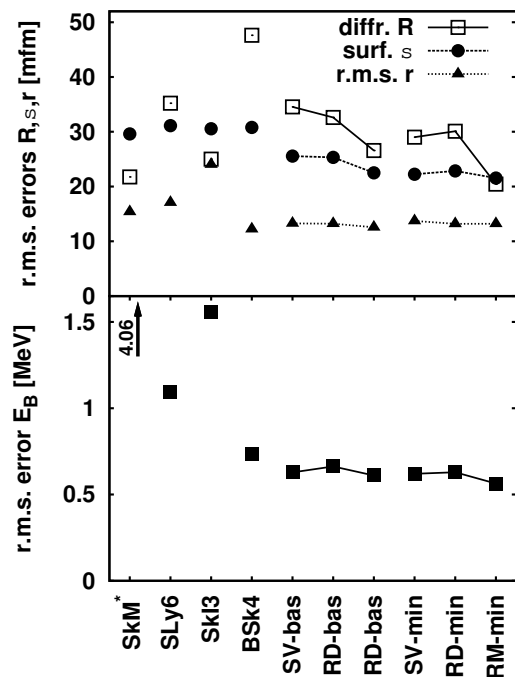


FIG. 1: Average errors on nuclear bulk properties for a variety of parameterizations as indicated. The errors are obtained from averaging over the reference set of SV-min [10]. Lower panel: errors on binding energy. Upper panel: errors on diffraction radius R , surface thickness σ , r.m.s. radius r .

gain is rather small. From the perspective of quality on bulk properties the new density dependence is neither harmful nor particularly advantageous. It is an equivalent alternative having the formal advantage to invoke only integer powers of density. It remains to be investigated how the new parameterizations perform in other respects.

B. Nuclear matter properties

Figure 2 shows result for nuclear matter properties. The lowest panel shows the incompressibility $K = 9 \rho^2 \partial_\rho^2 (E/A)$ where $(E/A)(\rho)$ is the bulk binding of symmetric matter per nucleon. The predictions are about the same for all forces. This isoscalar property is rather well determined by the wide span of nuclear sizes in all fit data. The extrapolation uncertainty is dramatically much larger for the new density dependence (compare SV with RD and RM). This is due to the larger flexibility of the new functional which has two parameters instead of one in the old density model. The form of density dependence can have a large influence on the bulk incompressibility. The new functional would allow to adjust much different values for K if there is a need to do so. The effective mass shows great variations for the traditional parameterizations. The larger data sets of the new adjustments (including BSk4) allow to determine its value

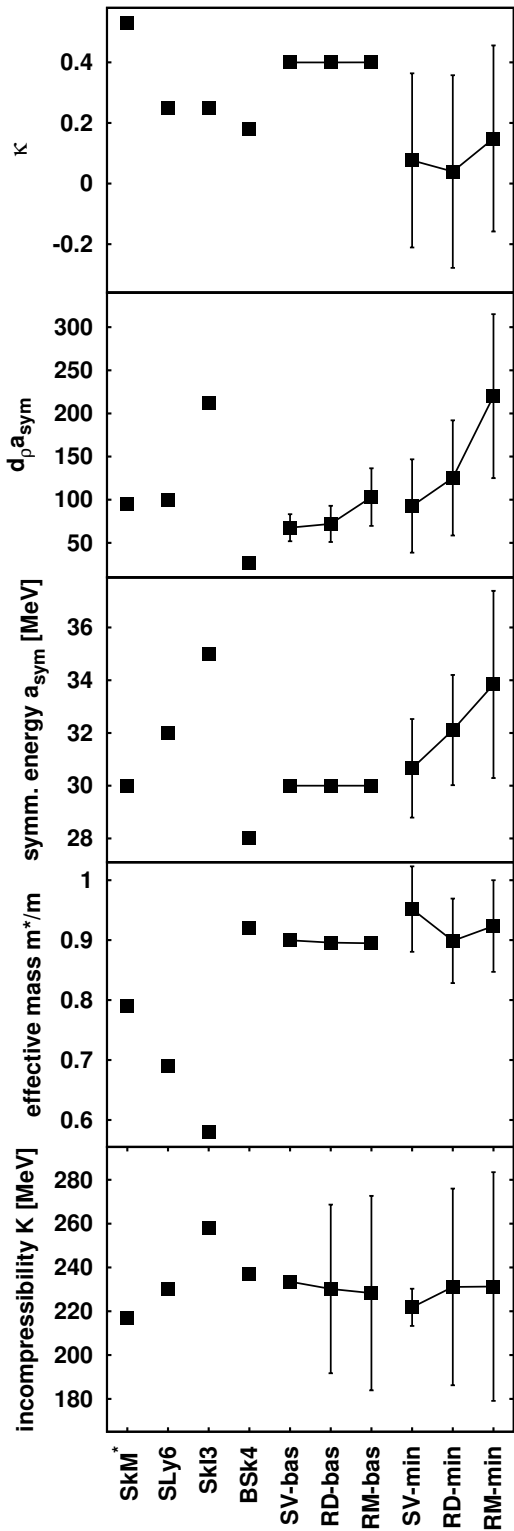


FIG. 2: Nuclear matter properties (filled boxes) together with their extrapolation uncertainty for the selected parameterizations.

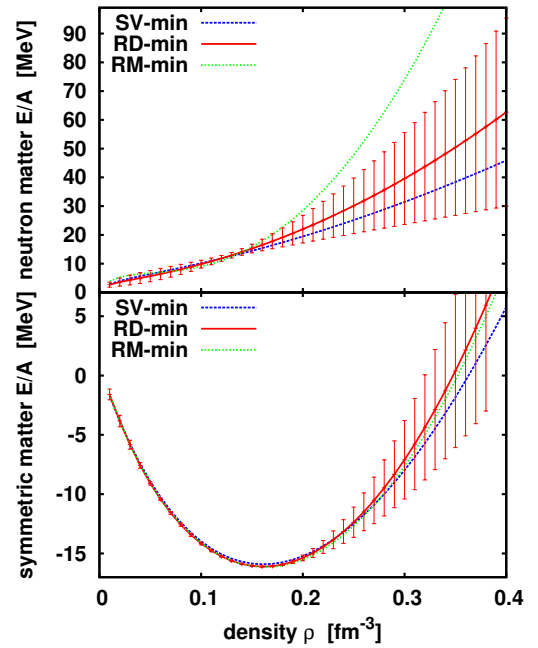


FIG. 3: (*Color online*) Binding energy per nucleon in homogeneous nuclear matter as function of density Lower: for symmetric matter. Upper: for neutron matter. Shown are results for the “min” parameterizations as indicated. Those for the “bas” parameterizations are very similar. The values for RD-min are given together with errors bars representing the uncertainty in the extrapolation.

in a rather narrow window close to $m^*/m = 0.9$. The “bas” parameterizations do not show error bars because the value was fitted. The free fits in the “min” parameterizations confirm the choice with a rather small uncertainty. This $m^*/m = 0.9$ is fortunately also the value which allows a good description of the giant quadrupole resonance.

All isovector properties (upper three panels) have large uncertainties in the unconstrained fits (“min” series). Moreover, their mean value differs visibly from the constrained values which explains the degrading of χ^2 when switching to the constrained fits (see figure 1). It is noteworthy that the extended density dependence in RM-min leads also to some enhancement of uncertainties in the isovector properties. The effect, however, is moderate in view of the freedom offered by the b_3, b'_3 terms in the density-dependent contribution (1e).

Figure 3 shows the binding energy curves in homogeneous nuclear matter for SV-min using the traditional density dependence and for RD-min as well as RM-min with the new functional. All three parameterization predict practically the same energies for low and normal nuclear densities, up to about $\rho = 0.28 \text{ fm}^{-3}$ for symmetric matter and up to about $\rho = 0.15 \text{ fm}^{-3}$ for neutron matter. These are the densities which are explored in finite nuclei and it is gratifying to see that the same information entering different models produce the same predic-

tions in the relevant range of density. However, the extrapolation to high densities shows significant differences. Very large effects are seen for RM-min in neutron matter due to the more flexible isovector parameterization. The difference in predictive power is nicely signaled by the extrapolation uncertainties deduced from the least-squares techniques. The error bands remain small in the region of low and normal nuclear density and quickly enhance for higher densities. The figure shows only the uncertainties for RD-min. The error band has the same trend for all parameterizations. It is in magnitude much the same for RM-min, but a factor of five smaller for SV-min. This difference indicates that the new density dependence, having two free parameters instead of one, allows more flexibility to adjust the equation of state in a broad density range. Unfortunately, the presently available empirical data do not allow to exploit this flexibility. It may be interesting to invoke results from ab-initio calculations to determine the density dependence more uniquely.

C. Giant resonances

Figure 4 shows the peak frequencies for the three basic giant resonances in ^{208}Pb . The resonance spectra were computed with the random-phase approximation done self-consistently with the same Skyrme interaction as was used for the ground state, for technical details see [34, 35]. The peak positions were deduced from an average over the resonance region covering ± 2 MeV around the peak. The GMR comes out very similar and similarly correct for all parameterizations. New are the huge uncertainties for all new parameterizations with the rational density dependence (RD and RM forces). This results is much similar to the results for the incompressibility in figure 2. The similarity is not surprising because it is known that incompressibility and GMR are closely related to each other [36]. The GDR behaves very similar with old and new density-dependence. Unconstrained fits (right-most three entries in the middle panel) yield too low peak frequencies and large uncertainties while constrained fits perform well by construction. There is an intimate relationship between GDR and the symmetry energy a_{sym} as well as the sum rule enhancement factor κ . The larger symmetry energies together with lower κ in figure 2 correlate with the lower GDR energies in figure 4. The GDR in ^{16}O , however, remains troublesome as it was for all previous SHF parameterizations [10, 12, 37]. The resonance energy stays far below the experimental values. Even the extended density dependence using b_3, b'_3 with their larger isovector freedom does not resolve the puzzle. The GQR (upper panel in figure 4) is known to have clear relation to the effective mass m^*/m [23]. This is also found in the present results (when comparing with m^*/m in figure 2). The results for the RD and RM forces are the same as for the SV forces. This shows that there is no influence from density dependence on the GQR.

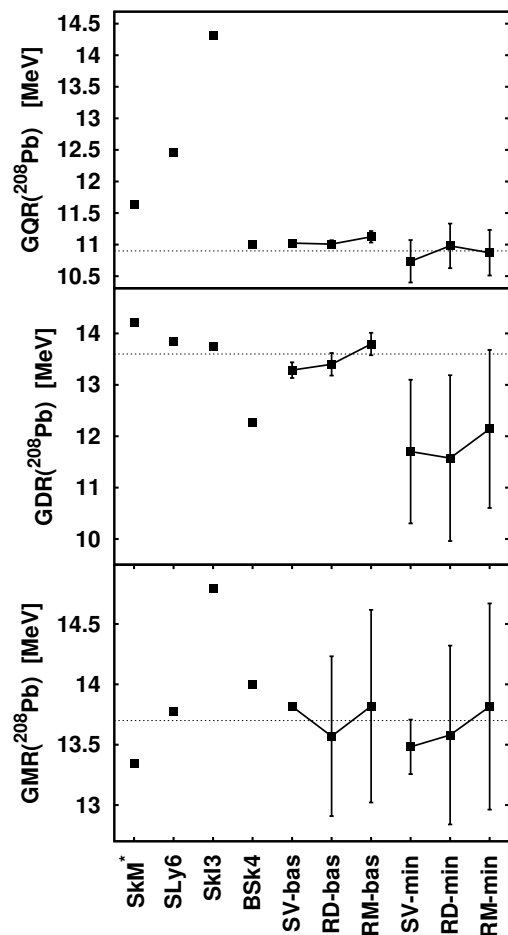


FIG. 4: Average peak energies of giant resonance excitations in ^{208}Pb . Lower panel: isoscalar giant monopole resonance (GMR); middle panel: isovector giant dipole resonance (GDR), upper panel: isoscalar giant quadrupole resonance (GQR). For the newly fitted forces, we show as error bars also the uncertainties in the prediction. The faint horizontal lines indicate the experimental resonance positions (taken from [31–33]).

The value $m^*/m \approx 0.9$ delivers a good reproduction of the GQR.

D. Super-heavy elements (SHE)

Figure 5 shows results for super-heavy elements (SHE). The results of the new parameterizations stay close to those of SV-bas and SV-min. The new density dependence makes little difference, mainly a slight growth of the uncertainty. Even then the uncertainties remain small. As a consequence, the mismatch of binding energy in the known SHE ^{264}Hs persists [12]. We deduce from the result that this mismatch is probably not related to an insufficient density dependence and thus cannot be cured by more flexible density profiles.

Another important observable in SHE are fission bar-

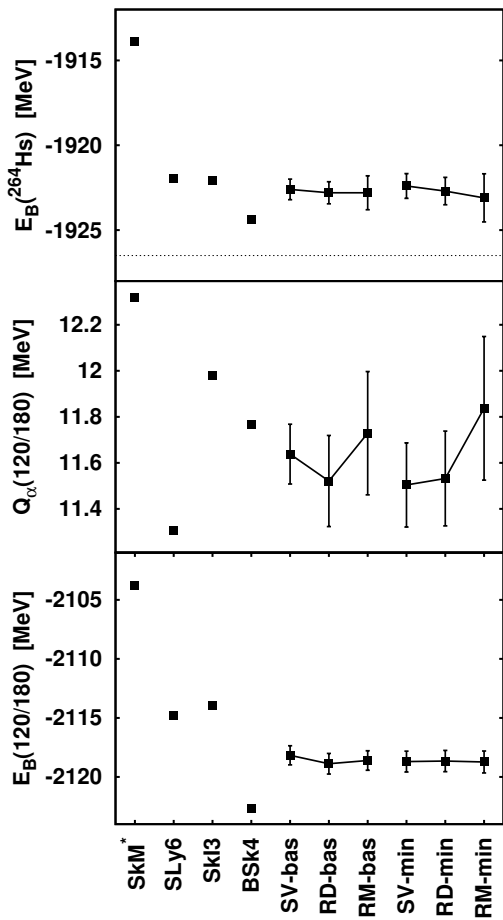


FIG. 5: Properties of super-heavy elements (boxes) together with their extrapolation uncertainty for the selected parameterizations. Lower: binding energy of the nucleus $Z = 120$, $N = 180$. Middle: Q_α value for the nucleus $Z = 120$, $N = 180$. Upper: binding energy of ^{264}Hs (including a correction for the rotational zero-point energy [10]), the experimental value is indicated by a dashed horizontal line [38].

riers. Figure 6 shows results for barriers of two groups of SHE, at the lower end Rf, Sg, Hs and more heavily $Z=112,114$ all calculated with the new density dependences, with the traditional one, and compared with experimental values [39, 40]. The predictions from the three forces shown in the figure are very much the same. The parameterizations SV-min, RD-min, and RM-min would also coincide and are not shown to keep the plot overseasable. The modified density dependence does not make any difference on fission barriers. The agreement is generally satisfying. Note, however, that the experimentally observed trend of fission barriers cannot be reproduced correctly by any SHF parameterization. The barriers are somewhat overestimated at the light side and underestimated in the heavier group. The same mismatch in the trend was found also for all conventional forces like SkI3 or SLy6 and for fission life-times [12]. The error bars indicated in the figure are as large as the deviation, for

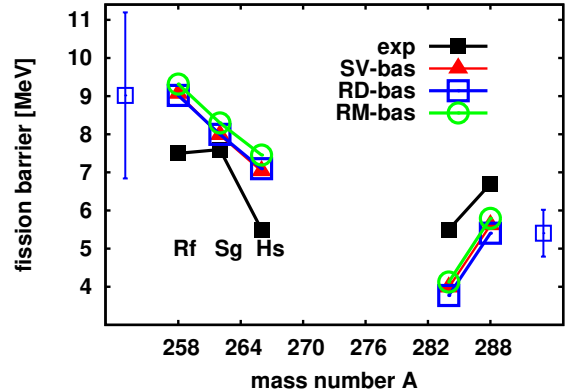


FIG. 6: (Color online) Fission barriers (filled boxes) of two groups of SHE for the selected parameterizations together with the experimental values. The extrapolation errors are very similar for all three forces. They are indicated for the lower group near the left margin and for the upper group near the right margin.

the lighter SHE even larger. This nourishes some hope that the trend could be resolved by appropriate retuning of the forces.

E. Energy systematics

Figure 7 shows the systematics of errors of binding energies $E_B^{(\text{SHF})} - E_B^{(\text{exp})}$ for all known even-even nuclei and for the forces SV-bas, RD-bas, and RM-bas. The results for SV-min, RD-min, and RM-min look very similar and are thus not shown here. The pattern in figure 7 are practically the same for all three forces: there is perfect agreement for the fit nuclei, there is good agreement for all nuclei with $A < 180$ when noting that the soft nuclei (the remaining group, neither fit nuclei nor deformed) acquire additional binding from correlation effects. A systematic trend to under-binding of heavy deformed nuclei is observed. The mismatch already seen for the case of ^{264}Hs in figure 5 was only one spotlight out of this trend. Similar as in [10] we have tried to improve the performance for energies by including deformed nuclei into the fit data set. This did improve the situation a bit, however, at the price of a much degraded overall quality. We find again that density dependence is not the key to the solution of this puzzle.

IV. CONCLUSIONS

In this paper, we have proposed and investigated an alternative form for the density dependent term in the Skyrme functional. The traditional form $\propto \rho^{2+\alpha}$ is replaced by a rational function $\propto (\alpha_{\text{inv}}\rho + \beta_{\text{inv}}\rho^2)/(1 + \alpha_{\text{inv}}\rho)$. The advantage of the new form is that it em-

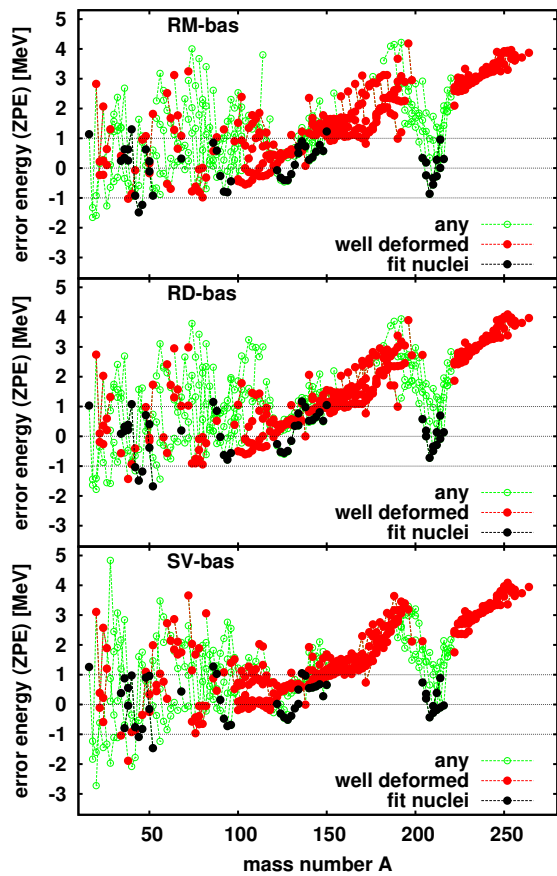


FIG. 7: (*Color online*) Systematics of binding energies over all known even-even nuclei for three parameterizations as indicated. Fit nuclei are indicated by filled black circles, well deformed one by filled red circles, and all remaining one by open green circles.

employs only integer powers of ρ and that it is analytical, except for one simple pole at $\rho = -\alpha_{\text{inv}}^{-1}$. The new form is thus applicable for projection schemes as, e.g., angular momentum, center-of-mass projection and particle number projection. We have also explored an extended form of the functional with one more density dependent term allowing for more flexibility in tuning isovector density-dependent terms. We have optimized the new functionals by adjustment to phenomenological data in standard manner and we have explored the properties of the newly developed functional in comparison to a couple of traditional Skyrme functionals. The straightforward methods of least-squares fitting allow also to deduce uncertainties on the predictions drawn from the fitted functionals.

The new forces provide at once an overall quality on standard nuclear bulk properties (energy, r.m.s. radius, diffraction radius, surface thickness) which is at least as good as the one obtained with the standard functional using exactly the same fitting data. The extended parameterization even provides a slight improvement. We have then checked the predictions for a couple of other nuclear observables, nuclear matter at equilibrium, gi-

ant resonance, super-heavy elements, fission, and energy systematics. The predictions in all these observables are very similar for both new functionals as compared to the recent fit within the standard Skyrme functional.

Slight differences appear for the uncertainties in the extrapolations. The new parameterizations, leaving more degrees of freedom, tend to produce larger extrapolation errors in some observables. In particular, the errors on incompressibility and giant monopole resonance are significantly larger. The extended new parameterization, having more isovector flexibility, produces slightly larger uncertainties in isovector observables as, e.g., the symmetry energy.

Large differences shows up for the equation-of-state of homogeneous matter at large densities, particularly for neutron matter. This is not so surprising because the form of density dependence is different. The complement of the observation is, in fact, very satisfying. There is practically no difference seen in the range of low and normal nuclear densities. This means that the adjustment to finite nuclei has managed to accommodate the region of normal densities in spite of the different form of the functionals.

Acknowledgment: This work was supported by BMBF under contract no. 06 ER 142D.

APPENDIX A: DENSITIES AND CURRENTS

The densities and currents are defined as

$$\begin{aligned}
 \rho_q(\vec{r}) &= \sum_{\alpha \in q} f_\alpha v_\alpha^2 |\varphi_\alpha(\vec{r})|^2 \\
 \tau_q(\vec{r}) &= \sum_{\alpha \in q} f_\alpha v_\alpha^2 |\nabla \varphi_\alpha(\vec{r})|^2 \\
 \vec{j}_q(\vec{r}) &= \Im m \left\{ \sum_{\alpha \in q} f_\alpha v_\alpha^2 \varphi_\alpha^+(\vec{r}) \nabla \varphi_\alpha(\vec{r}) \right\} \\
 \vec{\sigma}_q(\vec{r}) &= \sum_{\alpha \in q} f_\alpha v_\alpha^2 \varphi_\alpha^+(\vec{r}) \hat{\sigma} \varphi_\alpha(\vec{r}) \\
 \vec{J}_q(\vec{r}) &= -i \sum_{\alpha \in q} f_\alpha v_\alpha^2 \varphi_\alpha^+(\vec{r}) \nabla \times \hat{\sigma} \varphi_\alpha(\vec{r}) \\
 \xi_q(\vec{r}) &= \sum_{\alpha \in q} f_\alpha u_\alpha v_\alpha |\varphi_\alpha(\vec{r})|^2
 \end{aligned} \tag{A1}$$

where q labels the nucleon species with $q = p$ for protons and $q = n$ for neutrons. A density without an isospin label corresponds to a total density, i.e. $\rho = \rho_p + \rho_n$ and similarly for the other densities. The v_α and u_α are the standard BCS amplitudes, v_α for occupation and u_α the complementing one for non-occupation such that $v_\alpha^2 + u_\alpha^2 = 1$. The f_α is a phase-space weight which serves to provide a smooth cutoff of the space of single-particle states included in pairing. We use here a soft cutoff profile such as, $f_\alpha = [1 + \exp((\epsilon_\alpha - (\epsilon_F + \epsilon_{\text{cut}}))/\Delta\epsilon))]^{-1}$ where typically $\epsilon_{\text{cut}} = 5 \text{ MeV}$ and $\Delta\epsilon = \epsilon_{\text{cut}}/10$ [41, 42]. This works very well for all stable and moderately exotic nuclei. For better extrapolation ability away from the

	RD-bas	RD-min	RM-bas	RM-min
b_0	-1116.30	-1116.34	-1117.47	-1116.13
b'_0	-1127.16	-977.786	-1911.40	-1705.29
b_1	15.0000	14.4966	15.0000	10.5256
b'_1	72.8588	-18.9894	71.7330	16.5372
b_2	110.515	112.249	109.873	109.771
b'_2	-284.614	-317.996	-81.9695	-107.028
b_3			-9.64712	9.95249
b'_3			-4997.66	-7137.87
α			1.00000	1.00000
\tilde{b}_3	4364.93	4364.74	4395.28	4394.86
\tilde{b}'_3	3325.54	4218.63	15058.7	16756.7
α_{inv}	15.1299	15.1269	15.2122	15.3502
β_{inv}	16.9485	17.0715	16.5759	17.1909
b_4	63.0960	55.6340	64.4335	61.3840
b'_4	36.3802	52.0100	33.5588	38.4206
$V_{\text{pair,p}}$	658.539	685.826	708.671	820.390
$V_{\text{pair,n}}$	601.751	654.283	642.556	740.647
$\rho_{0,\text{pair}}$	0.203601	0.194093	0.194622	0.176469
$\frac{\hbar}{2m_p}$	20.7498207			
$\frac{\hbar}{2m_n}$	20.7212601			
e^2	1.44			
η_{tls}	1			
η_{Cex}	0			

TABLE II: The parameters of the Skyrme functional (1c) for the four new parameterizations.

valley of stability, the fixed margin ϵ_{cut} may be modified to use a band of fixed particle number $\propto N^{2/3}$ instead of

a fixed energy band [43].

APPENDIX B: DETAILS OF THE PARAMETERS

Table II provides the parameters of the four new parameterizations discussed in this paper. Dimensions of length are given in fm and dimensions of energy in MeV. This means: $b_0, b'_0 \leftrightarrow [\text{MeV fm}^3]$, $b_1, b'_1, b_2, b'_2 \leftrightarrow [\text{MeV fm}^5]$, $b_3, b'_3, \tilde{b}_3, \tilde{b}'_3 \leftrightarrow [\text{MeV fm}^6]$, $b_4, b'_4 \leftrightarrow [\text{MeV fm}^5]$, $\alpha, \alpha_{\text{inv}}, \beta_{\text{inv}} \leftrightarrow \text{fm}^3$, $e^2 \leftrightarrow [\text{MeV fm}]$, $\frac{\hbar^2}{2m} \leftrightarrow [\text{MeV fm}^2]$, and η_{tls} is a dimensionless switch factor.

The parameters b_i and b'_i used in the definition (1c) of the Skyrme functional are chosen to give a most compact formulation of the functional. The traditional form of the Skyrme functional is derived from an effective two-body interaction using force parameters t_i and exchange parameters x_i [1, 6, 20, 23]. There is a one-to-one correspondence of the parameters which reads

$$\begin{aligned}
b_0 &= t_0(1 + \frac{1}{2}x_0) , \\
b'_0 &= t_0(\frac{1}{2} + x_0) , \\
b_1 &= \frac{1}{4} [t_1(1 + \frac{1}{2}x_1) + t_2(1 + \frac{1}{2}x_2)] , \\
b'_1 &= \frac{1}{4} [t_1(\frac{1}{2} + x_1) - t_2(\frac{1}{2} + x_2)] , \\
b_2 &= \frac{1}{8} [3t_1(1 + \frac{1}{2}x_1) - t_2(1 + \frac{1}{2}x_2)] , \\
b'_2 &= \frac{1}{8} [3t_1(\frac{1}{2} + x_1) + t_2(\frac{1}{2} + x_2)] , \\
b_3 &= \frac{1}{4}t_3(1 + \frac{1}{2}x_3) , \\
b'_3 &= \frac{1}{4}t_3(\frac{1}{2} + x_3) , \\
b_4 &= \frac{1}{2}t_4 .
\end{aligned} \tag{B1}$$

-
- [1] M. Bender, P.-H. Heenen, and P.-G. Reinhard, *Rev. Mod. Phys.* **75**, 121 (2003).
- [2] J. Dechargé and D. Gogny, *Phys. Rev.* **C21**, 1568 (1980).
- [3] P.-G. Reinhard, *Rep. Prog. Phys.* **52**, 439 (1989).
- [4] P. Ring, *Prog. Part. Nucl. Phys.* **37**, 193 (1996).
- [5] J. W. Negele and D. Vautherin, *Phys. Rev.* **C5**, 1472 (1972).
- [6] J. Stone and P.-G. Reinhard, *Prog. Part. Nucl. Phys.* **58**, 587 (2007).
- [7] M. Samyn, S. Goriely, P.-H. Heenen, J. M. Pearson, and F. Tondeur, *Nucl. Phys.* **A700**, 142 (2002).
- [8] G.F. Bertsch, B. Sabbey, , and M. Uusnakki, *Phys. Rev. C* **71**, 054311 (2005).
- [9] T. Lesinski, M. Bender, K. Bennaceur, T. Duguet, and J. Meyer, *Phys. Rev. C* **76**, 014312 (2007).
- [10] P. Klüpfel, P.-G. Reinhard, T. J. Bürvenich, and J. A. Maruhn, *Phys. Rev. C* **79**, 034310 (2009).
- [11] M.V. Stoitsov, J. More, W. Nazarewicz, J. C. Pei, J. Sarich, N. Schunck, A. Staszczak, and S.Wild, *J. Phys.: Conf. Series* **180**, 012082 (2009).
- [12] J. Erler, P. Klüpfel, and P.-G. Reinhard, *J. Phys. G* **37**, 064001 (2010).
- [13] D. Vautherin and D. M. Brink, *Phys. Lett.* **32B**, 149 (1970).
- [14] J. Bartel, P. Quentin, M. Brack, C. Guet, and H.-B. Håkansson, *Nucl. Phys.* **A386**, 79 (1982).
- [15] S. Weisgerber and P.-G. Reinhard, *Phys. Lett. A* **158**, 407 (1991).
- [16] U. Serra, F. Garcias, M. Barranco, J. Navarro, and N. VanGiai, *Z. Phys. D* **20**, 277 (1991).
- [17] J. Dobaczewski, M. Stoitsov, W. Nazarewicz, and P.-G. Reinhard, *Phys. Rev. C* **76**, 054315 (2007).
- [18] P. Ring and P. Schuck, *The Nuclear Many-Body Problem* (Springer-Verl., New York, Heidelberg, Berlin, 1980).
- [19] G. Colo, H. Sagawa, S. Fracasso, and P. F. Bortignon, *Phys. Lett. B* (2007).
- [20] Y. M. Engel, D. M. Brink, K. Goeke, S. J. Krieger, and D. Vautherin, *Nucl. Phys.* **A249**, 215 (1975).
- [21] U. Post, E. Wust, and U. Mosel, *Nucl. Phys.* **A437**, 274 (1985).
- [22] J. Dobaczewski and J. Dudek, *Phys. Rev.* **C52**, 1827 (1995), erratum in *Phys. Rev.* **C55**, 3177 (1997).
- [23] M. Brack, C. Guet, and H.-B. Håkansson, *Phys. Rep.* **123**, 275 (1985).

- [24] J. Friedrich and N. Vögler, Nucl. Phys. **A373**, 192 (1982).
- [25] P. Klüpfel, P.-G. Reinhard, and J. Maruhn, Eur. Phys. J A **37**, 343 (2008),
- [26] J. Friedrich and P.-G. Reinhard, Phys. Rev. C **33**, 335 (1986).
- [27] P.-G. Reinhard and W. Nazarewicz, Phys. Rev. C **81**, 051303 (2010),
- [28] E. Chabanat, P. Bonche, P. Haensel, J. Meyer, and R. Schaeffer, Nucl. Phys. **A635**, 231 (1998), Nucl. Phys. **A643**, 441(E).
- [29] P.-G. Reinhard and H. Flocard, Nucl. Phys. **A584**, 467 (1995).
- [30] S. Goriely, M. Samyn, M. Bender, and J. M. Pearson, Phys. Rev. C **68**, 054325 (2003).
- [31] A. van der Woude, in *Electric and Magnetic Giant Resonances in Nuclei*, edited by J. Speth (World Scientific, 1991), vol. International Review of Nuclear Physics, Vol. 7, pp. 99–232.
- [32] A. Veyssiere, H.Beil, R.Bergere, P. Carlos, and A. Lepretre, Nucl. Phys. A **159**, 561 (1970).
- [33] T. C. team, `cdfe.sinp.msu.ru/services` (2007).
- [34] P.-G. Reinhard and Y. K. Gambhir, Ann. Phys. (Leipzig) **1**, 598 (1992).
- [35] P.-G. Reinhard, Ann. Phys. (Leipzig) **1**, 632 (1992).
- [36] J. P. Blaizot, Phys. Rep. **64**, 171 (1980).
- [37] P.-G. Reinhard, Nucl. Phys. A **649**, 305c (1999).
- [38] S. Hofmann and G. Münzenberg, Rev. Mod. Phys. **72**, 733 (2000).
- [39] J. Péter, Eur. Phys. J. A **22**, 271 (2004).
- [40] M. G. Itkis, Y. T. S. Oganessian, and V. I. Zagrebaev, Phys. Rev. C **65**, 044602 (2002).
- [41] P. Bonche, H. Flocard, P.-H. Heenen, S. J. Krieger, and M. S. Weiss, Nucl. Phys. **A443**, 39 (1985).
- [42] S. J. Krieger, P. Bonche, H. Flocard, P. Quentin, and M. S. Weiss, Nucl. Phys. **A517**, 275 (1990).
- [43] M. Bender, K. Rutz, P.-G. Reinhard, and J. A. Maruhn, Eur. Phys. J. **A8**, 59 (2000).